MATERIALS SCIENCE

10.1126/sciadv.1501492

Experimental test of Landauer's principle in single-bit operations on nanomagnetic memory bits

Jeongmin Hong,[1] Brian Lambson,[2] Scott Dhuey,[3] Jeffrey Bokor[1]*

Minimizing energy dissipation has emerged as the key challenge in continuing to scale the performance of digital computers. The question of whether there exists a fundamental lower limit to the energy required for digital operations is therefore of great interest. A well-known theoretical result put forward by Landauer states that any irreversible single-bit operation on a physical memory element in contact with a heat bath at a temperature T requires at least $k_BT\ln(2)$ of heat be dissipated from the memory into the environment, where k_B is the Boltzmann constant. We report an experimental investigation of the intrinsic energy loss of an adiabatic single-bit reset operation using nanoscale magnetic memory bits, by far the most ubiquitous digital storage technology in use today. Through sensitive, high-precision magnetometry measurements, we observed that the amount of dissipated energy in this process is consistent (within 2 SDs of experimental uncertainty) with the Landauer limit. This result reinforces the connection between "information thermodynamics" and physical systems and also provides a foundation for the development of practical information processing technologies that approach the fundamental limit of energy dissipation. The significance of the result includes insightful direction for future development of information technology.

INTRODUCTION

In 1961, Landauer (*1*) proposed the principle that logical irreversibility is associated with physical irreversibility and further theorized that the erasure of information is fundamentally a dissipative process. Among several seminal results, his theory states that for any irreversible single-bit operation on a physical memory element in contact with a heat bath at a given temperature, at least $k_BT\ln(2)$ of heat must be dissipated from the memory into the environment, where k_B is the Boltzmann constant and T is temperature (*2*). The single-bit reset operation process is schematically shown in Fig. 1A. As shown by Landauer (*1*, *2*), the extracted work from the process, regardless of the initial state of the bit, is $W_{operation} \geq k_BT\ln(2)$. This energy, $k_BT\ln(2)$, corresponds to a value of 2.8 zJ (2.8×10^{-21} J) at 300 K. In the field of ultra-low-energy electronics, computations that approach this energy limit are of considerable practical interest (*3*).

The first direct experimental test of Landauer's principle was reported in 2012 using a 2-μm glass bead in water manipulated in a double-well laser trap as a model system (*4*), and a higher precision measurement using 200-nm fluorescent particles in an electrokinetic feedback trap was recently reported (*5*). Although the topic is of great importance for information processing, the Landauer limit in single-bit operations has yet to be tested in any other physical system (*5*, *6*), particularly one that is relevant in practical digital devices. Therefore, confirming the generality of Landauer's principle in another, very different physical system is of great interest. Landauer and Bennett (*1*, *7*) both used nanomagnets as prototypical bistable elements in which the energy efficiency near the fundamental limits was considered. Accordingly, we report here an experimental study of Landauer's principle directly in nanomagnets.

[1]Electrical Engineering and Computer Sciences, University of California, Berkeley, Berkeley, CA 94720, USA. [2]Haynes and Boone LLP, 525 University Avenue, Palo Alto, CA 94301, USA. [3]The Molecular Foundry, Lawrence Berkeley National Laboratory, 1 Cyclotron Road, Berkeley, CA 94720, USA.
*Corresponding author. E-mail: jbokor@eecs.berkeley.edu

The fact that mesoscopic single-domain magnetic dots comprising more than 10^4 individual spins can nevertheless behave as a simple system with a single informational degree of freedom has been explicitly analyzed and confirmed theoretically and experimentally (*8*, *9*). Further theoretical studies (*10*, *11*) in which the adiabatic "reset to one" sequence for a nanomagnet memory suggested by Bennett (*7*) was explicitly simulated using the stochastic Landau-Lifschitz-Gilbert formalism, confirmed Landauer's limit of energy dissipation of $k_BT\ln(2)$ with high accuracy. For a nanomagnetic memory bit, magnetic anisotropy is used to create an "easy axis" along which the net magnetization aligns to minimize magnetostatic energy. As shown in Fig. 1A, the magnetization can align either "up" or "down" along the easy axis to represent binary "0" and "1." We denote the easy axis as the y axis. The orthogonal x axis is referred to as the "hard axis." The anisotropy of the magnet creates an energy barrier for the magnetization to align along the hard axis, allowing the nanomagnet to retain its state in the presence of thermal noise. To reset a bit stored in the nanomagnet, magnetic fields along both the x and y axes are used. The x axis field is used to lower the energy barrier between the two states, and the y axis field is then used to drive the nanomagnet into the 1 state.

RESULTS

In the micromagnetic simulations of Lambson and Madami (*10*, *11*), and as shown in Fig. 1B, the reset sequence can be divided into four steps. Initially, the nanomagnet is in either 0 or 1 state, and afterward, it is reset to the 1 state. The internal energy dissipation in the nanomagnet is found by integrating the area of m-H loops for magnetic fields applied along both the x and y axes (hard and easy axes, respectively) followed by their subtraction. To perform the hysteresis loop measurements of interest, the external magnetic fields are specified as a function of time in a quasistatic manner as illustrated in Fig. 1B.

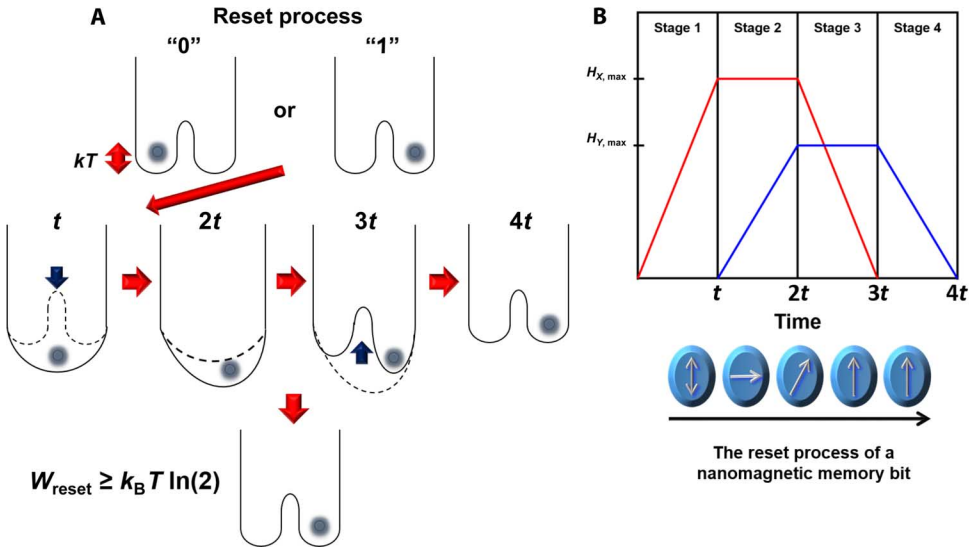

Fig. 1. Thermodynamics background. (**A**) Description of single-bit reset by time sequence. Before the erasure, the memory stores information in state 0 or 1; after the reset, the memory stores information in state 0 in accordance with the unit probability. (**B**) Timing diagram for the external magnetic fields applied during the restore-to-one process. H_x is applied along the magnetic hard axis to remove the uniaxial anisotropy barrier, whereas H_y is applied along the easy axis to force the magnetization into the 1 state. Illustrations are provided of the magnetization of the nanomagnet at the beginning and end of each stage and of the direction of the applied field in the *x*-*y* plane.

Applying the fields in this manner splits the operation into four stages, and during any given stage, one of the fields is held fixed while the other increased linearly from zero to its maximum value or vice versa, as shown in Fig. 1B. In stage 1, H_x is applied to saturate the hard axis, which removes the energy barrier and ensures that the energy dissipation is independent of the barrier height.

As explained by Bennett (*7*), whether the Landauer erasure operation is classified as reversible or irreversible depends on whether the initial state of the nanomagnet is truly unknown (that is, randomized) or known. However, in both the reversible and irreversible cases, the amount of energy transfer that occurs during the operation is $k_B T \ln(2)$. The distinction between reversible and irreversible lies in whether or not the operation can be undone by applying the fields depicted in Fig. 1B in reverse. A more complete discussion is contained in Bennett's work (*7*). Accordingly, for experimental purposes, there is no need to randomize or otherwise specially prepare the initial state of the nanomagnets to observe the $k_B T \ln(2)$ limit. This can be further justified by observing that the first stage of the reset operation depicted in Fig. 1B (applying a field along the *x* axis) is symmetric with respect to the initial orientation of the nanomagnets along the *y* axis. After the first stage, there is no remaining *y* axis component of the magnetization of the nanomagnets, so subsequent stages of the operation are independent of the initial orientation of the nanomagnets along the *y* axis. As a result, the amount of energy dissipated during the Landauer erasure operation does not depend on the initial state of the nanomagnet.

Magneto-optic Kerr effect (MOKE) in the longitudinal geometry was used to measure the in-plane magnetic moment, *m*, of a large array of identical Permalloy nanomagnets, whereas the magnetic field, *H*, was applied using a two-axis vector electromagnet. The experimental setup is shown in Fig. 2A. The lateral dimensions of the nanomagnets were less than 100 nm to ensure they were of single domain, whereas the spacing between magnets was 400 nm to avoid dipolar interactions between magnets yet provide sufficient MOKE signal. Scanning electron microscopy (SEM) images of the sample are shown in Fig. 2B. Magnetic force microscopy (MFM) was used to confirm that the nanomagnets have a single-domain structure and have sufficient anisotropy to retain state at room temperature, as shown in Fig. 2C. Longitudinal MOKE is sensitive to magnetization along only one in-plane direction (*9*), so the sample was mounted on a rotation stage, and separate measurements were made with the sample oriented to measure *m* along each of the easy and hard axes of the nanomagnets. For each measurement along the two orientations, the magnetic field along the axis of MOKE sensitivity was slowly (time scale of many seconds) ramped between positive and negative values, whereas the transverse magnetic field (perpendicular to the axis of MOKE sensitivity) was held at fixed values. The values of the transverse magnetic field were selected to generate *m*-*H* curves corresponding to each of the four steps of the reset protocol shown in Fig. 1B. The comprehensive hysteresis loops during the complete erasure process are illustrated schematically in video S1.

To quantitatively determine the net energy dissipation during the reset operation from the MOKE data, it is necessary to calibrate both the applied magnetic field and the absolute magnetization of the nanomagnets. The applied field was measured using a three-axis Hall probe sensor. To calibrate the MOKE signal, the total moment, $M_S V_T$, for the full sample was measured using a vibrating sample magnetometer (VSM). M_S is the saturation magnetization for the full sample and V_T is the total volume of the magnetic layer on the sample. An example of experimental results from one run is shown in Fig. 3. The volume of each nanomagnet, *V*, and the number of nanomagnets on the substrate were measured and calibrated using SEM for the lateral dimensions and count, and atomic force microscopy (AFM) was used to determine the thickness (see the Supplementary Materials for details). In this way, the $M_S V$ value for an individual nanomagnet from the MOKE data could be absolutely determined.

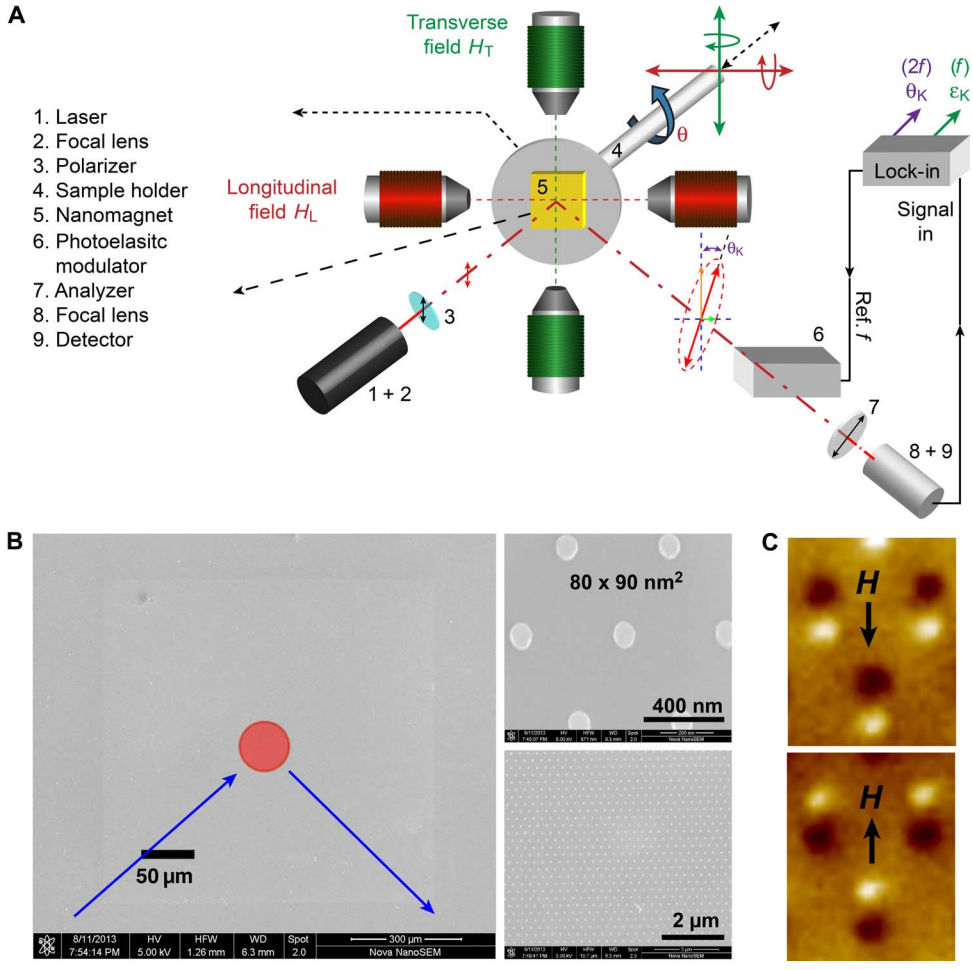

Fig. 2. The magneto-optic Kerr microscopy experimental set up. (**A**) Schematic of the experimental MOKE setup. (**B**) SEM images of the sample. The circle represents the approximate size of the probe laser spot. (**C**) MFM images of individual single-domain nanomagnets.

The energy dissipation (the magnetization energy transferred by the applied magnetic field to a nanomagnet) is determined by the total area of the hysteresis curves. As seen in Fig. 3 and video S1, the *x* and *y* hysteresis curves are traversed in opposite directions during the course of the reset operation so that the total energy is found by subtracting the area of the *y* hysteresis (easy axis) loop from the area of the *x* hysteresis (hard axis) loop. Further details concerning the calculation of energy dissipation are given in the Supplementary Materials.

As expected, the temperature dependence between 300 and 400 K was very similar to the theoretical prediction based on the average of all 2000 simulations. The mean energy dissipation was found to be 0.6842 k_BT, which corresponds to a 95% confidence interval of 0.6740 to 0.6943 k_BT. These values are in very close agreement with the Landauer limit, $k_BT\ln(2)$. The experimental energy dissipation was measured at temperatures varying from 300 to 400 K. As seen in fig. S1, the hysteresis loops for both axes individually show a clear systematic temperature dependence that is consistent with micromagnetic simulations (*10*, *11*), but the temperature dependence of the measured net energy dissipation was smaller than the run-to-run variation, as seen in Fig. 4A. For the set of runs, the energy dissipation was measured to be (4.2 ± 0.9) zJ, which corresponds to a value of (1.0 ± 0.22)k_BT (for T = 300 K). Statistical experimental results for energy dissipation are shown in Fig. 4B. As explicitly demonstrated by Lambson and Madami (*10*, *11*), for "ideal" nanomagnets, the dissipation should average exactly to $k_BT\ln(2)$ with a small run-to-run variation caused by thermal fluctuations. The average dissipation for five trials at room temperature was measured to be (6.09 ± 1.43) zJ at T = 300 K. This is consistent with a value of (1.45 ± 0.35)k_BT, which is extremely close to the Landauer limit of $k_BT\ln(2)$ or 0.69 k_BT. The quoted error was determined by combining in quadrature the uncertainties in each of the measured variables: nanomagnet area and thickness, magnetic field calibration, magnetic moment, lithographic variation, and the statistical variation among the five trials.

A small remanent magnetization was typically observed in the hard axis (*x*) direction (curves in Fig. 3 do not pass through the origin). We attribute this to fabrication variations among the nanomagnets. When the symmetry axes of the individual nanomagnets are not perfectly aligned with the axes of the applied magnetic fields, each of their remanent easy axis magnetizations will have a small component along the hard axis direction. Because of fabrication variations, there will be a distribution of misalignments. Experiments involving small rotations of the sample to find the net symmetry axis and measure the effect of a net tilt of the array with respect to the magnetic field axes are described in the Supplementary Materials. On the basis of these

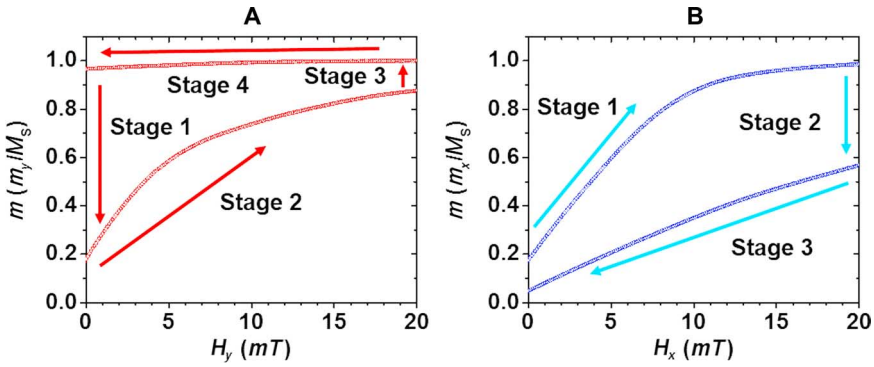

Fig. 3. The experimental *m-H* hysteresis loops of nanomagnets during the reset operation. (**A** and **B**) The m_y-H_y loop (easy axis) (A) and the m_x-H_x loop (hard axis) (B). The indicated stages correspond to the timing diagram shown in Fig. 1B.

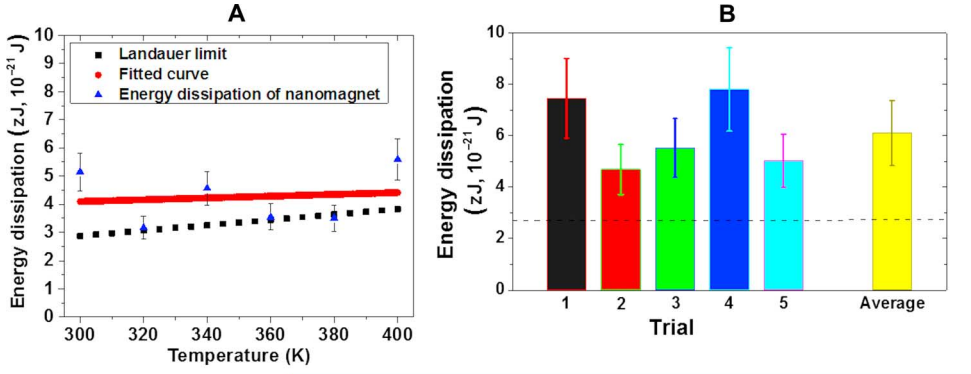

Error	Area	Thickness	H_{calib}	M_S	Lithography	Trials	Total
%	1.2	7.9	1	10	8.2	14.3	20.8

Fig. 4. Experimental results for total energy dissipation. (**A**) The temperature dependence of energy dissipation during single-bit reset. Triangles represent experimental data obtained from integrating and subtracting hysteresis loops similar to the example shown in Fig. 3. The red line is the best fit to the experimental data. The black squares represent the Landauer limit, $k_BT\ln(2)$. (**B**) The experimentally determined energy dissipation during the reset operation. Different bars from 1 to 5 represent separate experimental runs to measure energy dissipation. The values in the table indicate estimated relative SD of the measurements of average dot area (Area), average dot thickness (Thickness), applied magnetic field (H_{calib}), saturation magnetization (M_S), residual remanence due to "tilt" effect (Lithography), and the run-to-run variation (Trials), respectively. The total experimental error was determined from the root-mean-square value for all of the variables in the table. The dotted line represents the Landauer limit, $k_BT\ln(2)$ for $T = 300$ K.

experiments, we estimate the magnitude of random variation of the symmetry axes of the nanomagnets across the array to be approximately ±1°, which is roughly consistent with the observed remanence (see also simulation in fig. S4C). We estimate that the small excess energy dissipation above the Landauer value that we observed in our experiment can be mainly attributed to this effect (see discussion in the Supplementary Materials). Other possible sources of excess dissipation include domain motion and pinning by defects and edge roughness (*12*, *13*) and edge effects. The effects of dot shape and subdomain structure on energy dissipation are explicitly considered in the simulations reported by Madami *et al.* (*11*). At this time, it is not feasible to separately estimate the magnitude of these various contributions to the small excess energy dissipation observed in our experiments. However, the fact that our results depart by only 50 to 100% of the Landauer value strongly indicates that these Permalloy nanomagnets behave very closely to the ideal "single-spin" magnets and therefore provide a practical and viable system for further exploration of the ultimate energy dissipation in information processing. As an example, a nanomagnetic logic gate for demonstrating reversible logic operation with dissipation below the Landauer limit was analyzed theoretically by Lambson *et al.* (*10*). Our results suggest that such an experiment is indeed feasible.

DISCUSSION

We have experimentally measured for the first time the intrinsic minimum energy dissipation during a single-bit operation using a nanoscale digital magnetic memory bit. Our result is within 2 SDs of the value of $k_BT\ln(2)$ predicted by Landauer. Although experimental tests of Landauer's limit have previously been performed using trapped microbeads, our result using a completely different physical system confirms its generality and, in particular, its applicability to practical information processing systems. Any practical nanomagnetic memory or logic device will inevitably involve additional energy loss

associated with the actuation mechanism (that is, the external applied magnetic fields in this experiment); however, our results demonstrate the potential to approach Landauer's limit in future information processing systems. Therefore, the significance of this result is that today's computers are far from the fundamental limit and that future marked reductions in power consumption are possible with further development of nanomagnetic memory and logic devices. Given that power consumption is the key issue that limits the continued improvement in digital computers, the result has profound suggestions for the future development of information technology.

MATERIALS AND METHODS

Fabrication of nanomagnetic memory bits

We fabricated an array of identical, single-domain, noninteracting, elliptically shaped nanomagnets by lift-off patterning of an electron beam (e-beam) evaporated amorphous Permalloy (NiFe) film on a silicon substrate using e-beam lithography. The base pressure of the e-beam evaporator was 2×10^{-7} torr, and the film thickness was 10 nm. The sample was fabricated at The Molecular Foundry at Lawrence Berkeley National Laboratory.

Dimensional metrology of nanomagnet islands using SEM and scanning probe microscopy

SEM images were collected with a Carl Zeiss LEO 1550. The statistical errors of area of the magnet and thickness measurements were 1.2 and 7.9%, respectively. The image analysis was performed using ImageJ software from the National Institutes of Health. The average size of magnets was calculated with the software and calibrated to the highly accurate average pitch of the nanomagnet array produced by the e-beam lithography tool (Vistec VB300). The thickness of the nanomagnets was determined with AFM performed in noncontact mode using the Veeco Dimension 3100 system. MFM measurements using the same instrument were conducted in a dynamic-lift mode with a lift-off distance of 30 nm.

Magneto-optic Kerr spectroscopy

To perform high-resolution magneto-optic Kerr spectroscopy, we used a focused MOKE system in lateral mode. A 635-nm diode laser was directed toward the sample, which was located between the poles of a vector magnet. The laser spot size on the sample was approximately 50 μm, covering approximately 10^4 nanomagnets. However, the magnetic field at the probe spot was calibrated by a three-axis Hall probe sensor (C-H3A-2m Three Axis Magnetic Field Transducer, SENIS GmbH). The accuracy of the magnetic field measurement is estimated at ~1%. The time to sweep full hysteresis loops was 20 min (1 Oe/s).

Energy dissipation calculation

The energy dissipation was calculated by the following equation

$$\begin{aligned}\int M \cdot \mathrm{d}H &= \int \{(M_x \times \mathrm{d}H_x) + (M_y \times \mathrm{d}H_y)\} \\ &= \int (M_x \times \mathrm{d}H_x) + \int (M_y \times \mathrm{d}H_y) \\ &= \mathrm{Area}_{m_x\text{-}H_x\mathrm{loops}} + \mathrm{Area}_{m_y\text{-}H_y\mathrm{loops}}\end{aligned}$$

The measured value of the energy dissipation is not dependent on the laser spot size/shape or the number of nanomagnets illuminated by the spot. This is because the saturation magnetization M_S and the average spin moment for the nanomagnets μ ($=M_S V$) of each individual magnet were separately measured as described below. The magnetization as measured by MOKE was calibrated by setting the saturated value of the MOKE signal to this average saturated spin moment, μ.

SUPPLEMENTARY MATERIALS

Supplementary material for this article is available at http://advances.sciencemag.org/cgi/content/full/2/3/e1501492/DC1

Fig. S1. The temperature dependence of the magnetization curves as measured by MOKE on both the easy and hard axes.

Fig. S2. *m-H* loops of the total magnetic moment of the full sample.

Fig. S3. (A) Hard axis *m-H* curves corresponding to stage 1 of the Landauer erasure protocol with various sample tilt angles.

Fig. S4. (A) The simulated energy dissipation at 0 K by varying the maximum fields ($H_{x,\ max}$ and $H_{y,\ max}$) field.

Video S1. The comprehensive hysteresis loops during the complete erasure process.

References (*14*–*16*)

REFERENCES AND NOTES

1. R. Landauer, Irreversibility and heat generation in the computing process. *IBM J. Res. Dev.* **5**, 183–191 (1961).
2. R. Landauer, Dissipation and noise immunity in computation and communication. *Nature* **335**, 779–784 (1988).
3. J. D. Meindl, J. A. Davis, The fundamental limit on binary switching energy for terascale integration (TSI). *IEEE J. Solid-St. Circ.* **35**, 1515–1516 (2000).
4. A. Bérut, A. Arakelyan, A. Petrosyan, S. Ciliberto, R. Dilenshneider, E. Lutz, Experimental verification of Landauer's principle linking information and thermodynamics. *Nature* **484**, 187–189 (2012).
5. Y. Jun, M. Gavrilov, J. Bechhoefer, High-precision test of Landauer's principle in a feedback trap. *Phys. Rev. Lett.* **113**, 190601 (2014).
6. T. Sagawa, Thermodynamics of information processing in small systems. *Prog. Theor. Phys.* **127**, 1–56 (2012).
7. C. H. Bennett, The thermodynamics of computation—A review. *Int. J. Theor. Phys.* **21**, 905–940 (1982).
8. S. Salahuddin, S. Datta, Interacting systems for self-correcting low power switching. *App. Phys. Lett.* **90**, 093503 (2007).
9. D. A. Allwood, G. Xiong, M. D. Cooke, R. P. Cowburn, Magneto-optical Kerr effect analysis of magnetic nanostructures. *J. Phys. D Appl. Phys.* **36**, 2175–2182 (2003).
10. B. Lambson, D. Carlton, J. Bokor, Exploring the thermodynamic limits of computation in integrated systems: Magnetic memory, nanomagnetic logic, and the Landauer limit. *Phys. Rev. Lett.* **107**, 010604 (2011).
11. M. Madami, M. d'Aquino, G. Gubbiotti, S. Tacchi, C. Serpico, G. Carlotti, Micromagnetic study of minimum-energy dissipation during Landauer erasure of either isolated or coupled nanomagnetic switches. *Phys. Rev. B* **90**, 104405 (2014).
12. D. C. Jiles, D. L. Atherton, Ferromagnetic hysteresis. *IEEE Trans. Magn.* **19**, 2183–2185 (1983).
13. D. A. Allwood, G. Xiong, C. C. Faulkner, D. Atkinson, D. Petit, R. P. Cowburn, Magnetic domain-wall logic. *Science* **309**, 1688–1692 (2005).
14. B. Lee, J. Hong, N. Amos, I. Dumer, D. Litvinov, S. Khizroev, Sub-10-nm-resolution electron-beam lithography toward very-high-density multilevel 3D nano-magnetic information devices. *J. Nanopart. Res.* **15**, 1665 (2013).
15. Z. Gu, M. E. Nowakowski, D. B. Carlton, R. Storz, M.-Y. Im, J. Hong, W. Chao, B. Lambson, P. Bennett, M. T. Alam, M. A. Marcus, A. Doran, A. Young, A. Scholl, J. Bokor, Sub-nanosecond signal propagation in anisotropy-engineered nanomagnetic logic chains. *Nat. Commun.* **6**, 6466 (2015).
16. R. V. Telesnin, E. N. Ilyicheva, N. G. Kanavina, N. B. Stepanova, A. G. Shishkov, Domain-wall motion in thin permalloy films in pulsed magnetic field. *IEEE Trans. Magn.* **5**, 232–236 (1969).

Acknowledgments

Funding: We acknowledge financial support from the NSF Center for Energy Efficient Electronics Science under award no. 0939514. The work at The Molecular Foundry (TMF) was supported by the U.S. Department of Energy, Office of Basic Energy Sciences, Division of Materials Sciences and Engineering under contract no. DE-AC02-05CH11231. **Author contributions:** J.B. supervised

the project. J.H. and B.L. established and performed MOKE experiments and simulation. J.H. performed AFM/MFM and SEM measurements and error analyses. S.D. fabricated nanomagnets using e-beam lithography. J.H., B.L., and J.B. wrote the manuscript with input from all authors. **Competing interests:** The authors declare that they have no competing interests. **Data and materials availability:** All data needed to evaluate the conclusions in the paper are present in the paper and/or the Supplementary Materials. Data related to this paper may be requested from the authors.

Submitted 20 October 2015
Accepted 19 January 2016
Published 11 March 2016
10.1126/sciadv.1501492

Citation: J. Hong, B. Lambson, S. Dhuey, J. Bokor, Experimental test of Landauer's principle in single-bit operations on nanomagnetic memory bits. *Sci. Adv.* **2**, e1501492 (2016).

ScienceAdvances
AAAS

Experimental test of Landauer's principle in single-bit operations on nanomagnetic memory bits

Jeongmin Hong, Brian Lambson, Scott Dhuey and Jeffrey Bokor

(March 11, 2016)
Sci Adv 2016, 2:.
doi: 10.1126/sciadv.1501492